

Determining bed boundaries from inversion of EM logging data using general measures of model structure and data misfit

Zhiyi Zhang*, Raghu K. Chunduru*, and Michael A. Jervis†

ABSTRACT

In this paper we propose a new method to locate bed boundaries by carrying out a 1-D nonlinear inversion of electromagnetic (EM) logging data. We first solve for 1-D resistivity structure in which the earth is modeled using layers of constant thickness. This thickness is determined based upon the tool resolution and the desired resolution from the user. We use general measures of data misfit and model structure in the inversion to construct piecewise-constant models through the iteratively reweighted least-squares (IRLS) procedure, and we minimize a generic global model objective function subject to data constraints. The general measure includes the traditional l_p norm as a special case. The recovered piecewise-constant models simulate traditional models comprised of a few uniform layers and hence permit easy determination of bed boundaries. The generic model objective function allows the incorporation of prior geological information and provides measures of the closeness to the reference model and the amount of structure in the recovered model. We develop an efficient scheme to incorporate the IRLS procedure into the search for the appropriate regularization parameter at each iteration. The iterations required by the IRLS algorithm are computed in a more efficient manner for the piecewise-constant models. The applicability of the algorithm is demonstrated using synthetic and field data.

INTRODUCTION

Electromagnetic (EM) logging data are functions of resistivity structure and geometry factors such as the length of invasion zones and layer boundaries. Inversion techniques can provide information about subsurface geological structures. In a typical 2-D inversion of resistivity logging data, the earth is modeled, utilizing the cylindrical coordinate system, as the bore-

hole, the invaded zone, and the virgin zone. Theoretically, the inversion may recover both the geometric parameters (borehole diameter, invasion length, bed boundaries, etc.) and the resistivity value for each zone. However, the geometric and resistivity parameters have different physical units and affect the data in fundamentally different ways. Moreover, the equivalence between geometric and resistivity parameters results in nonunique models, which are difficult to recover simultaneously. One way to reduce the nonuniqueness and cut the computational cost of 2-D inversions is to determine the bed boundary positions before performing the inversion and then to keep the boundaries fixed during the inversion. This method has been widely used in the logging industry with success. Most existing boundary-picking algorithms use inflection points of the input data curves. These algorithms are computationally efficient but in many cases may not meet the required accuracy for 2-D inversions. In this paper, we propose an alternative way to detect bed boundaries through 1-D vertical inversion of resistivity logging data. In this vertical 1-D inversion the earth is modeled using horizontal layers parallel to the surface of the earth, and the borehole effect is ignored.

One-dimensional vertical inversion using an l_2 norm has been addressed by several authors (Lin et al., 1984; Dyos, 1987; Freedman and Minerbo, 1991; Zhang et al., 1994). Recovered models from traditional least-squares solutions are usually smooth representations of the true models. This smoothness, however, does not facilitate accurate estimation of bed boundaries. Furthermore, an l_2 measure of misfit is not robust in the presence of outliers in the data. Therefore, we investigate the solutions of the nonlinear inverse problem using measures other than the typical l_2 norm. By judiciously choosing measures of data misfit and model structures, we build algorithms that are immune to outliers in the data and generate piecewise-constant models.

The use of robust measures of the data misfit in geophysical problems has led to significant improvements in EM data processing (Egbert and Booker, 1986; Chave et al., 1987; Chave and Thomson, 1989; Sutarno and Vozoff, 1991). A few authors

Manuscript received by the Editor April 2, 1998; revised manuscript received May 12, 1999.

*Baker Atlas, 10201 Westheimer, Bldg. 1A, Houston, Texas 77042. E-mail: ian.zhang@bakeratlas.com.

†Formerly Baker Atlas, 10201 Westheimer, Bldg. 1A, Houston, Texas 77042; currently Tomoseis Inc., 1650 W. Sam Houston Parkway, Houston, Texas 77043.

© 2000 Society of Exploration Geophysicists. All rights reserved.

General Measure Inversion

77

have also investigated the application of a non- l_2 measure of model structure in the solution of the nonlinear inverse problem. Dosso (1990) minimizes the l_1 norm of the vertical derivative of the model to construct piecewise-constant models for the 1-D magnetotelluric (MT) problem. He also uses an l_1 measure of misfit and solves the linearized inverse problem by using linear programming (LP). Oldenburg and Ellis (1993) and Ellis et al. (1993) use an l_1 measure to construct blocky models for the 2-D MT problem. These authors use LP to obtain their solutions. Farquharson and Oldenburg (1998) use an iteratively reweighted least-squares technique to solve the nonlinear inverse problem of transient EM data, where general measures of the model structure and misfit are used.

In this paper, we develop a new algorithm to determine bed boundaries and formation resistivity by solving a 1-D nonlinear inverse problem using general measures of model structure and data misfit. The traditional l_p norm can be considered a subset of this general measure. We use horizontal layers with constant thickness to model the earth. This thickness is determined by the desired resolution from the user and the resolution power of the logging tools. The resolution of the recovered bed boundaries is only as accurate as the chosen layer thickness. The bed boundaries are fixed during the inversion, and the constant but unknown resistivity value within each layer is recovered from the inversion. A global model objective function is minimized subject to data constraints, and the iteratively reweighted least-squares (IRLS) technique is used to solve the inverse problem. The algorithm is tested on both synthetic and field data.

METHODOLOGY

Induction tools consist of individual transmitter- and receiver-coil pairs. Responses from each transmitter-receiver pair can be summarized to generate the overall response from the tool. In induction logging, a signal generator produces an ac current, which is injected into the transmitter coil. The current in the transmitter establishes a primary magnetic field, which generates eddy currents in the earth. These eddy currents in turn induce a secondary magnetic field in the earth, which is a function of physical properties of the earth, and the receiver coils measure the voltages induced by the secondary magnetic field. The tool response is further converted to apparent resistivity defined as (Moran and Kunz, 1962)

$$\rho_a = \left[\frac{-4\pi L}{\omega^2 \mu_0^2} \sum_{i=1}^{N_T} \sum_{j=1}^{N_R} N_i^T N_j^R V_{ij} \right]^{-1}, \quad (1)$$

where N_i^T is the number of turns of the i th transmitter; N_j^R is the number of turns of the j th receiver; V_{ij} is the induced voltage received by the i th receiver from the j th transmitter with single turns; and N_T and N_R are the numbers of the transmitters and receivers, respectively. The value L is given by $1 / \sum_{i=1}^{N_T} \sum_{j=1}^{N_R} N_i N_j / L_{ij}$, where L_{ij} is the coil separation of the i th transmitter and the j th receiver. The final data are given in ohm-meters.

Since our intention is to detect the bed boundary, we are less concerned about the accuracy of the resistivity. Therefore, in the forward modeling, we neglect the borehole and invasion effects. This reduces the forward modeling to a 1-D problem, which is solved following the work of Anderson (1986) and Kennedy et al. (1986) for an arbitrarily oriented magnetic

dipole in a horizontal-layered earth. To locate the bed boundaries accurately, we model the earth with a relatively large number of layers of constant thickness. This thickness is determined according to the tool resolution or the desired resolution from the user.

A GENERAL MEASURE FOR VECTORS

A typical geophysical inverse problem involves minimizing a model objective function and/or a data misfit objective function. These model and data objective functions are obtained by taking the norms of the model structure vector and the data misfit vector, respectively. Different norms can be used as a measure of a vector, whether that vector defines the misfit between the observed and predicted data or describes a model. Consider a vector \mathbf{x} with elements x_j , $j = 1, 2, \dots, N$. The traditional l_p norm of \mathbf{x} is given by

$$\|\mathbf{x}\|^p = \sum_{j=1}^N |x_j|^p, \quad (2)$$

where $p \geq 1$. When $p = 2$ this expression is the l_2 norm of the vector. In this paper we propose a new measure

$$\|\mathbf{x}\|_\epsilon^p = \sum_{j=1}^N (x_j^2 + \epsilon^2)^{p/2}, \quad (3)$$

where $p > 0$ and $\epsilon \ll |x_j|$ is some positive number. We explain how to choose ϵ later using numerical examples. Zhang et al. (1998) have proven, from a statistical point of view, that p in equation (3) must be \geq zero. When $p \geq 1$, the above general measure reduces to the one proposed by Ekblom (1973, 1987) and used by Farquharson and Oldenburg (1997). As ϵ becomes small and $p \geq 1$, the measure in equation (3) tends to the l_p norm in equation (2).

The parameter p in the general measure controls weights on the elements of a vector. To illustrate this we create a vector $\mathbf{x} = (x_1, x_2, \dots, x_N)$, whose elements range from 10^{-3} to 18. We then compute $(x_j^2 + \epsilon^2)^{p/2}$ for all components of this vector with $p = 2, 1, 0.5$, and 0 (Figure 1). Here we set ϵ to a negligible value of 10^{-6} . As p decreases, the weights on small values of x_j increase and the weights for large values of x_j decrease. The

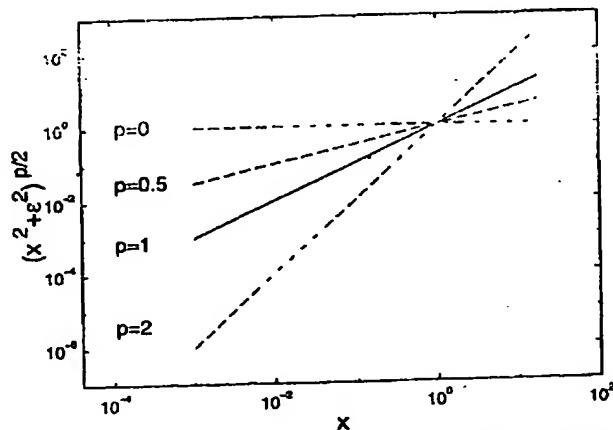


FIG. 1. Comparison of general measures with different values of p . The value of ϵ is 10^{-6} .

general measure is the sum of each $(x_j^2 + \epsilon^2)^{p/2}$, so the smaller p is, the more important the small components in $\|x\|_p^2$. Setting $p = 0$ leads to a uniform weighting, which equals 1 for all values of x_j . The resultant general measure equals the dimension of x . In this extreme case, all elements of x contribute the same toward the general measure $\|x\|_p^2$.

Until now, no attempt has been made in the literature to use equation (2) as a measure of misfit or model structure with $0 \leq p < 1$, where the l_p norm is not defined. From a numerical point of view, when $p < 1$ the derivative of $\|x\|_p^p$ has a singularity at $x_j = 0$, $1 \leq j \leq N$. Our general measure can be considered a perturbation and extension of the traditional l_p norm, and the singularity at $x_j = 0$, $1 \leq j \leq N$ is removed with the introduced small positive constant ϵ . Below, we use this general measure to develop our inversion algorithm.

INVERSION ALGORITHM

In the nonlinear inverse problem we are solving, the model $m(r)$ is the spatial distribution of resistivity of the earth, discretized as

$$m(r) = \sum_{j=1}^N m_j \psi_j(r), \quad (4)$$

where N is the number of the model parameters; r is the position vector; and ψ_j is the basis functions. In this paper, we choose ψ_j as boxcar functions. Suppose the forward modeling problem, which calculates the response from a given model, is expressed as

$$d^{\text{pre}} = f(m), \quad (5)$$

where $m = (m_1, m_2, \dots, m_N)^T$; d^{pre} is the data vector generated from this model; and f is the nonlinear mapping that connects the model space to the data space. The inverse problem consists of finding the model from the collection that reproduces the observed data to a desired misfit level, which is the most plausible given any prior geological and geophysical information.

Since this is a nonlinear inverse problem, we use linearization and iterate for the solution. The objective function to be minimized is

$$\Phi = \phi_m + \beta^{-1} \phi_d. \quad (6)$$

The model objective function is given by

$$\phi_m = \alpha \phi_s + (1 - \alpha) \phi_x, \quad (7)$$

where $\phi_s = \|W_s(m - m_{\text{ref}})\|_p^p$, and $\phi_x = \|W_x(m - m_{\text{ref}})\|_p^p$. The data objective function is given by

$$\phi_d = \|[W_d(d^{\text{obs}} - d^{n-1}) - J(m^{n-1})\delta m]\|_p^p - \phi_d^{\text{tar}}, \quad (8)$$

where d^{n-1} is the predicted data from m^{n-1} , the model from the previous iteration, and J is the sensitivity matrix,

$$J_{ij} = \frac{\partial d_i(m^{n-1})}{\partial m_j}, \quad (9)$$

where m_{ref} is the reference model that can be used to incorporate a priori geological information into the solution. The parameter ϕ_d^{tar} is the target misfit level at each iteration, which is reduced gradually—typically by a factor between 2 and 10—to prevent the violation of the linearization. The value β is the

regularization parameter. In equation (7), the two terms on the right side provide (a) the measure of the closeness of the recovered model to the reference model and (b) the amount of structure in the reconstructed model, respectively. The value W_s is the weighting matrix associated with the minimum-norm solution. In this paper, we assume the reference model is of equal importance over the entire spatial extent and thus choose the identity matrix as W_s . Since a minimum-norm solution may possess unwanted, detailed structures when noise exists in the data, a first-order, finite-difference operator W_x is used to minimize the amount of structure presented in the recovered model. The constant α controls the balance between the minimum-norm and minimum-structure solutions. When $\alpha = 0$ and $p = 2$, this is a least-squares solution that has the minimum model norm. The smoothing operator W_x can be introduced by setting $0 < \alpha < 1$, with W_d containing statistical information about the data. The noise in the data is assumed to be uncorrelated, so W_d is diagonal. If the noise is Gaussian with zero mean, then the diagonal elements of W_d are the reciprocals of the standard deviations.

To minimize the objective function in equation (7), we set $m = m^{n-1} + \delta m$, differentiate Φ with respect to the elements of δm , and equate the resulting equations to zero. The system of equations to be solved is given by

$$\begin{aligned} & [\alpha W_s^T R_s W_s + (1 - \alpha) W_x^T R_x W_x + \beta^{-1} J^T W_d^T R_d W_d] \delta m \\ & = \beta^{-1} J^T W_d^T R_d W_d (d^{\text{obs}} - d^{n-1}) \\ & + [\alpha W_s^T R_s W_s + (1 - \alpha) W_x^T R_x W_x] (m^{\text{ref}} - m^{n-1}), \end{aligned} \quad (10)$$

where R_s , R_x , and R_d are diagonal matrices whose elements are

$$(R_s)_{ii} = p(x_i^2 + \epsilon^2)^{p/2-1}, \quad (11)$$

$$(R_x)_{ii} = p(u_i^2 + \epsilon^2)^{p/2-1}, \quad (12)$$

and

$$(R_d)_{ii} = p(v_i^2 + \epsilon^2)^{p/2-1}, \quad (13)$$

where x_i , u_i , and v_i are the i th elements of the corresponding vectors $W_s(m - m_{\text{ref}})$, $W_x(m - m_{\text{ref}})$, and $W_d[d^{\text{obs}} - d(m^{n-1}) - J(m^{n-1})\delta m]$, respectively. The detailed derivation of equation (10) is given in the Appendix. We explain how to choose values of ϵ later using numerical examples. When p tends to zero, the system in equation (10) reduces to that without regularization because R_s and R_x are both zero matrices. If we introduce three diagonal matrices \hat{R}_s , \hat{R}_x , and \hat{R}_d so that $\hat{R}_s^T \hat{R}_s = R_s$, $\hat{R}_x^T \hat{R}_x = R_x$, and $\hat{R}_d^T \hat{R}_d = R_d$, then equation (10) can be simplified to

$$\begin{aligned} & [W_m^T \hat{W}_m + \beta^{-1} J^T \hat{W}_d^T \hat{W}_d J] \delta m \\ & = \beta^{-1} J^T \hat{W}_d^T \hat{W}_d (d^{\text{obs}} - d^{n-1}) + \hat{W}_m^T \hat{W}_m (m^{\text{ref}} - m^{n-1}), \end{aligned} \quad (14)$$

where $W_m = \alpha \hat{W}_s^T \hat{W}_s + (1 - \alpha) \hat{W}_x^T \hat{W}_x$, $\hat{W}_s = \hat{R}_s W_s$, $\hat{W}_x = \hat{R}_x W_x$, and $\hat{W}_d = \hat{R}_d W_d$. Since R_s , R_x , and R_d are all diagonal, \hat{R}_s , \hat{R}_x , and \hat{R}_d can be computed easily.

General Measure Inversion

79

Equation (14) is very similar to the system of equations that would be obtained if all measures in the objective function were sum-of-squares measures. The iterations required by the IRLS procedure have been absorbed into the iteration associated with the linearization of the nonlinear problem. At each iteration associated with the linearization of the problem, the system of equations given in equation (14) is constructed and solved using the reweighting matrices R_1 , R_2 , and R_3 computed from the model obtained from the previous iteration.

The regularization parameter β is determined in the following manner. Before the final desired misfit is achieved, we solve equation (14) at 2 to 4 logarithmically spaced values for β in a relatively small interval, usually between 0.001 and 100, at each iteration. We do not update matrices R_1 , R_2 , and R_3 in the line search. Once the final target misfit for the inversion is reached, the regularization parameter β is fixed and further iterations are carried out to allow the IRLS procedure to converge. The iteration is terminated when the change in the model norm reaches a predetermined value, usually set to 1%.

NUMERICAL EXAMPLES

In the following, we demonstrate the benefits of using generic measures of model structure and data misfit by applying the inversion to synthetic dual-phase induction log (DPIL) data generated over a two-layer resistivity model. The DPIL tool is a conventional induction logging tool that operates at 20 kHz. It consists of several transmitter-receiver pairs and provides medium and deep resistivity curves. Since the medium curve has higher vertical resolution, we use it for boundary picking. The true model and the synthetic medium curve for the model are shown in Figure 2. The data were generated for a single frequency of 20 kHz at a station interval of 0.1 m. For convenience, we refer to the simulated data from the true models in synthetic examples as the observed data and the data computed from the models recovered from the inversion as the predicted data.

In the inversion, the earth was parameterized into 100 layers of 0.1-m constant thickness. This thickness is determined from experiments and is about the limit of the resolution from the inversion of DPIL data. Such a parameterization not only allows us to determine the bed boundary locations accurately but

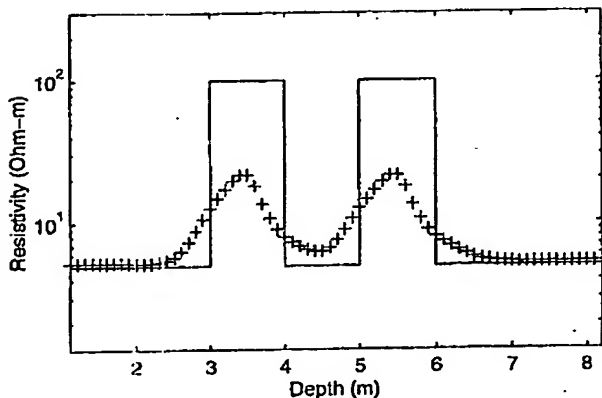


FIG. 2. The true model (the solid line) and the synthetic data to be used in the inversion (the crosses).

also provides us with a fine vertical variation of the resistivity structure. A starting model of a 5-ohm-m half-space was used for the following two examples. Such an initial model is easy to build. However, better starting models (if available) can be used to reduce the number of iterations in the inversion. The parameter α was chosen to be 0.002 based on our experience.

EM data are usually contaminated with noise. Two common types of noise are Gaussian noise and outliers. Our experience indicates that, while a small amount of Gaussian noise has little effect on inversions using general measures, outliers can affect inversions significantly. To illustrate the benefits of using robust measures of misfit, we perturbed two data samples in the synthetic data in Figure 2. The data values at 3 m and 8.2 m were changed from 10.56 to 20 ohm-m and 5.25 to 10 ohm-m, respectively.

We first inverted the perturbed data using l_2 measures as the model structure and data misfit. The best-fit solution was reached after eight iterations, which corresponds to a 6% rms error. The recovered model from the inversion (Figure 3a) has been affected severely by the two outliers in the data, and the overall structure is very rough. The shallower resistive zone has shifted upward, and an artificial resistive layer has been created between 8 and 8.5 m. The predicted data in Figure 3b are trying to fit these two outliers. This example highlights

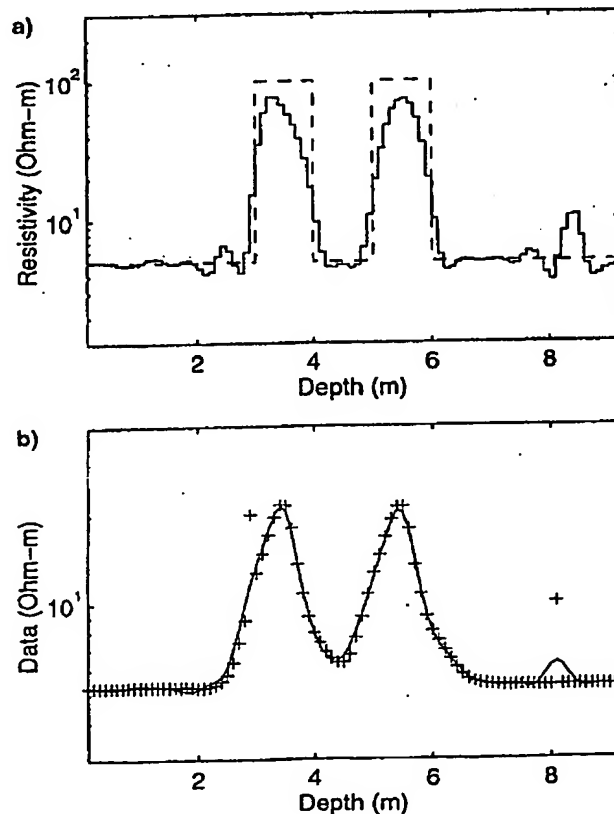


FIG. 3. Results from the inversion of the perturbed data using the l_2 norm. (a) The model. The solid line denotes the recovered model, and the dashed line denotes the true model. (b) The predicted (solid line) and observed (plus signs) data.

the vulnerability of an l_2 measure of misfit to outliers in the data.

We then test our algorithm using $p = 1$ on the same data set. First, we determine the values of ϵ for computing ϕ_s , ϕ_x , and ϕ_d in equations (7) and (8). These values of ϵ should be small enough so the final values of ϕ_s , ϕ_x , and ϕ_d will not differ significantly from their values with $\epsilon = 0$ yet large enough to make the IRLS procedure converge. Before carrying out the inversion, we do not know the final values of ϕ_s , ϕ_x , and ϕ_d necessary for determining values of ϵ . In a borehole environment, however, the observed data, which are given in apparent resistivity/conductivity, are a reasonable estimation of the true resistivity structure. Thus, we can use the data in Figure 2 to calculate ϕ_s , ϕ_x , and ϕ_d as functions of ϵ (Figure 4). From these three curves, we choose values of ϵ that are small enough so that ϕ_s , ϕ_x , and ϕ_d differ only in the third significant figure from their values with $\epsilon = 0$ yet are large enough to make the IRLS procedure converge. The values of ϵ for the model structure and for data misfit are set to 0.01 and 10^{-5} , respectively.

After 20 iterations, the best rms misfit of 6.5% is reached. Figure 5 shows the model and data from the inversion. The recovered model is an excellent representation of the true model. The two outliers in the observed data are, in effect, ignored by the predicted data. This indicates that the fit to the spiky data obtained using essentially an l_1 measure of misfit is more appropriate than that obtained using an l_2 measure. This example also indicates that the use of an l_1 measure of model structure can lead to more blocky models from the inversion.

To further test our algorithm, we apply it to a 2-D synthetic data set generated from a modified Oklahoma benchmark model shown in Figure 6. This model has a large range of layer thicknesses and resistivity values with conductive invasion. The synthetic data are generated at a sampling rate of four samples per foot for a DPIL tool. Data from 80 to 270 ft (24 to 82 m) are used in the inversion, and the subsurface is parameterized with 0.5-ft (0.15-m) thick layers. A 1-ohm-m half-space is used as both the starting model and the reference model in

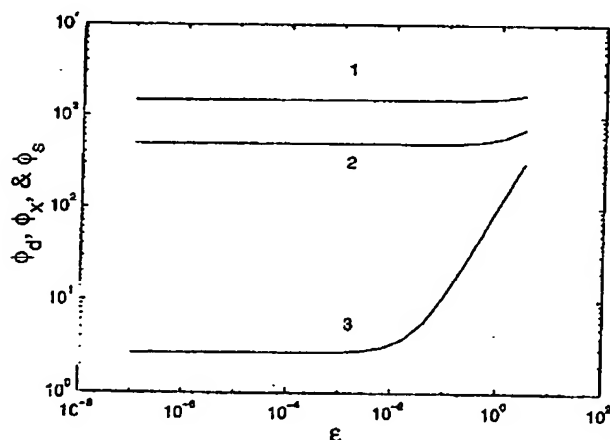


FIG. 4. The variation with ϵ of general measure (with $p = 1$) for ϕ_s (curve 1), ϕ_x (curve 2), and ϕ_d (curve 3) computed using the data in Figure 2.

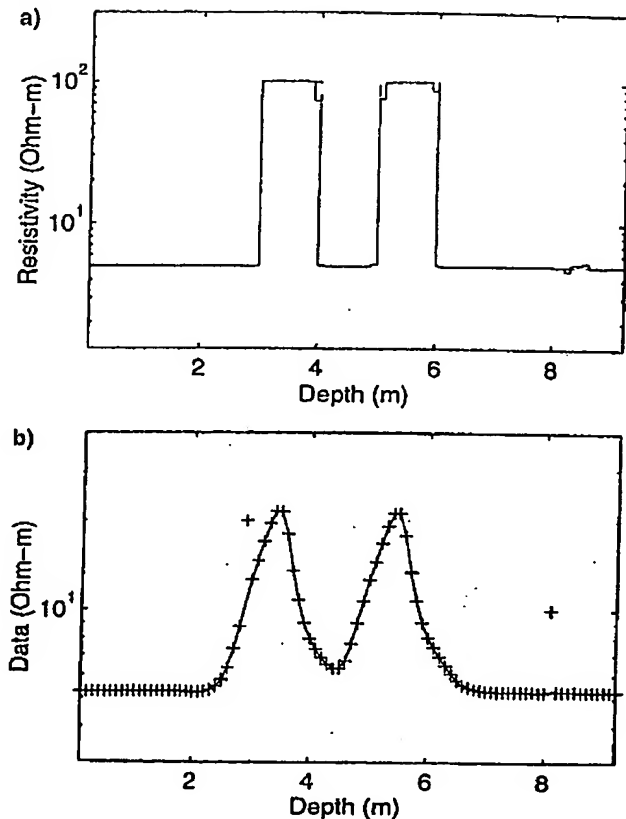


FIG. 5. Inversion of the perturbed data using a robust measure for the misfit and model structure. (a) Model. (b) Data.

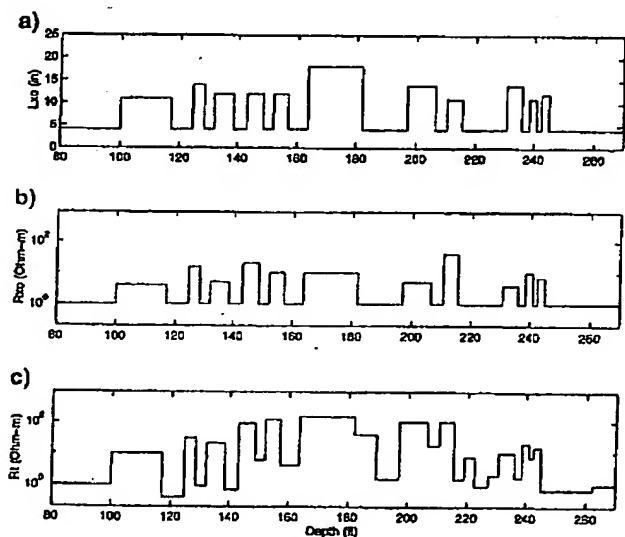


FIG. 6. Oklahoma benchmark model. (a) L_{20} (length of invasion). (b) R_{20} (resistivity of invasion). (c) R_f (resistivity of formation).

General Measure Inversion

81

ie inversion. The parameters α , p , and ϵ for the misfit and model structure are set to 0.002, 0.5, and 10^{-5} , respectively. A small threshold value of 0.001 is used for the change of model norm in the IRLS procedure to obtain maximum blockiness in the recovered model. After 20 iterations, the inversion converges to the final model in Figure 7a. The use of a general norm as the measure of model structure in the inversion enables the recovery of the piecewise-constant model, which in turn allows easy detection of the bed boundaries. The estimated resistivities are also close to the true resistivity values. Because of the resolution limitation of the deep curve, the inversion does not resolve the thin layers around 240 ft (73 m). The recovered resistivity model is an average of the invaded and true formation resistivity and hence differs from the true model. The predicted and observed data in Figure 7b agree within 5% rms error.

FIELD DATA EXAMPLE

As a field data example, we applied the proposed algorithm to the dual-phase induction data acquired from the Abu Dhabi region in the Middle East. In the inversion, we used the deep data from 8465 to 8600 ft (2580 to 2620 m), acquired at a sampling rate of four samples per foot. The subsurface was parameterized using 0.5-ft (0.15-m) layers and a starting resistivity of 1 ohm-m. Inversion was performed using $p = 0.5$, $\alpha = 0.002$, and an ϵ value of 10^{-4} for both misfit and model structure. In the line search, misfit evaluations were conducted at four logarithmically equispaced points between 0.001 and 100. The inversion was performed on the deep induction curve. There was an excellent data match between the field and the synthetic data obtained from the inversion (Figure 8b) to about 1% rms error. The final model obtained from the inversion in Figure 8a seemingly resolved most of the major formation layers.

CONCLUSIONS

The proper location of bed boundaries and good prior information about the resistivities of the formations, among various other factors, play a key role in the success of a 2-D resistivity inversion scheme. Conventionally, bed boundaries are located based on the slope variations in the borehole EM data. This may result in unrealistic bed boundaries, especially in regions of strong shoulder-bed effects. Inversion schemes can be used to estimate the bed boundary locations and to obtain accurate a priori information about resistivity for 2-D inversions.

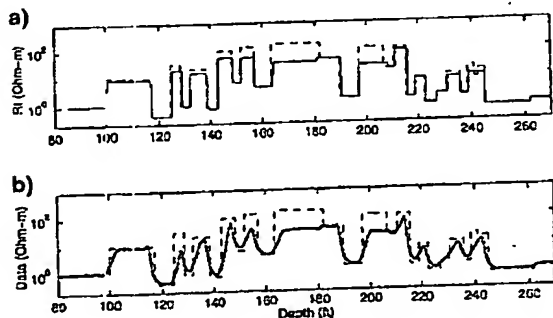


FIG. 7. (a) True (dashed line) and recovered (solid line) models. (b) Observed (dots) and predicted (solid line) data from the inversion of a 2-D deep induction curve.

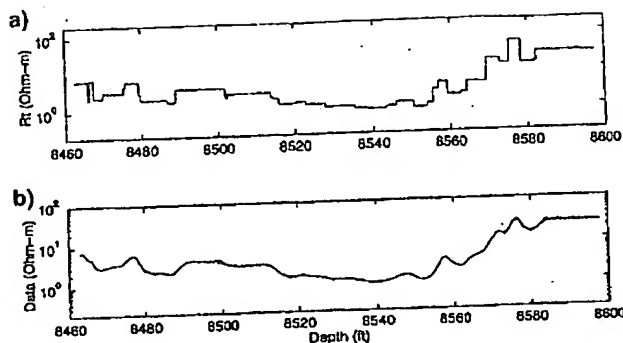


FIG. 8. Results from the inversion of an Abu Dhabi deep induction curve. (a) Recovered model. (b) Observed (dashed line) and predicted (solid line) data.

In this paper, we have developed and implemented a model-norm-based inversion algorithm using general measures of misfit and model structure, in which a generic global model objective function is minimized. A large number of thin layers were used to accommodate arbitrary variations of the geological structure. An iterative reweighted least-squares procedure was used in the inversion to generate a piecewise-constant model that allowed easy determination of bed boundaries. The results obtained from the synthetic and field data examples proved the effectiveness of the proposed scheme. The inversion of synthetic log data showed that our inversion algorithm can recover the bed boundaries and resistivity of the formations effectively, even in the presence of noise. Application of the algorithm on a field data example from the Middle East demonstrated the ability of the proposed inversion algorithm to recover the bed boundaries and resistivities of the formation from field data. Though the proposed algorithm is not a replacement for 2-D inversion, it provides excellent a priori information for the 2-D inversion. Also, in regions where the subsurface is one dimensional (no invasion present), the algorithm works effectively in estimating the resistivity variation of the subsurface.

REFERENCES

- Anderson, B., 1986, The analysis of some unsolved induction interpretation problems using computer modeling: 27th Ann. Logging Sympos., Soc. Prof. Well Log Analysts, paper H.
- Chave, A. D., and Thomson, D. J., 1989, Some comments on magnetotelluric response function estimation: *J. Geophys. Res.*, 94, 14215-14225.
- Chave, A. D., Thomson, D. J., and Ander, M. E., 1987, On the robust estimation of power spectra, coherences, and transfer functions: *J. Geophys. Res.*, 92, 633-648.
- Dosso, S. E., 1990, Inversion and appraisal for the one-dimensional magnetotellurics problem: Ph.D. thesis, Univ. of British Columbia.
- Dyos, C. J., 1987, Inversion of induction log data by the method of maximum entropy: 28th Ann. Log. Symp., Soc. Prof. Well Log Analysts, Transactions, T1-13.
- Egbert, G. D., and Booker, J. R., 1986, Robust estimation of geomagnetic transfer functions: *Geophys. J. Royal Astr. Soc.*, 87, 173-194.
- Eklom, H., 1973, Calculation of linear best l_1 -approximations: *BIT*, 13, 292-300.
- , 1987, The l_1 -estimate as limiting case of an l_p - or Huber-estimate, in Dodge, Y., Ed., *Statistical data analysis based on the l_1 -norm and related methods*: Elsevier Science Publ. Co., Inc.
- Ellis, R. G., Farquharson, C. G., and Oldenburg, D. W., 1993,

- Approximate inverse mapping inversion of the COPROD2 data: *J. Geomag. and Geoelec.*, 45, 1001-1002.
- Farquharson, C. G., and Oldenburg, D. W., 1998, Nonlinear inversion using general measures of data misfit and model structure: *Geophys. J. Internat.*, 134, 213-227.
- Freeman, R., and Minerbo, G. N., 1991, Maximum entropy inversion of induction log data: *SPE Formation Evaluation*, June, 259-268.
- Kernedy, W. D., Curry, S. M., Gill, S. P., and Morrison, H. F., 1986, Induction response in deviated boreholes: 27th Ann. Logging Sympos., Soc. Prof. Well Log Analysts, paper FTF.
- Liu, Y., Gianzero, S., and Strickland, R., 1984, Inversion of induction logging data using the least-squares technique: 25th Ann. Log. Symp., Soc. Prof. Well Log Analysts, AA1-14.

- Moran, J. H., and Kunz, K. S., 1962, Basic theory of induction logging and application to study of two-coil sondes: *Geophysics*, 27, 829-858.
- Oldenburg, D. W., and Ellis, R. G., 1993, Efficient inversion of magnetotelluric data in two dimensions: *Phys. Earth Plan. Int.*, 81, 177-200.
- Sutarno, D., and Vozoff, K., 1991, Phase-smoothed robust *M*-estimation of magnetotelluric impedance functions: *Geophysics*, 56, 1999-2007.
- Zhang, Y., Sheu, L. C., and Liu, C., 1994, Inversion of induction logs based on maximum flatness, maximum oil, and minimum oil algorithms: *Geophysics*, 59, 1320-1326.
- Zhang, Z., Mezzatesta, A. G., and Treitel, S., 1998, Bayesian inversion of resistivity logging data using a general pdf: 14th EM Workshop, Abstracts, 173.

APPENDIX A

DERIVATION OF EQUATION (10)

Consider the differentiation of the first term in equation (7). Let $\mathbf{x} = \mathbf{W}_s(\mathbf{m} - \mathbf{m}_{ref})$. Then the general measure of \mathbf{x} is

$$\begin{aligned} \|\mathbf{x}\|_{\epsilon}^p &= \sum_{i=1}^N (x_i^2 + \epsilon^2)^{p/2} \\ &= \sum_{i=1}^N \left\{ \left[\sum_{j=1}^N (W_s)_{ij} [m_j - (m_{ref})_j] \right]^2 + \epsilon^2 \right\}^{p/2} \end{aligned} \quad (\text{A-1})$$

Setting $\mathbf{m} = \mathbf{m}^{n-1} + \delta\mathbf{m}$ and differentiating the above equation lead to

$$\frac{\partial \|\mathbf{x}\|_{\epsilon}^p}{\partial \delta\mathbf{m}} = \mathbf{W}_s^T \mathbf{R}_s \mathbf{W}_s (\mathbf{m}^{n-1} + \delta\mathbf{m} - \mathbf{m}_{ref}), \quad (\text{A-2})$$

where \mathbf{R}_s is a diagonal matrix whose elements are given by

$$p \left\{ \left[\sum_{j=1}^N (W_s)_{ij} [m_j - (m_{ref})_j] \right]^2 + \epsilon^2 \right\}^{p/2-1} \quad (\text{A-3})$$

Identical reasoning leads to

$$\frac{\partial \|\mathbf{W}_x(\mathbf{m} - \mathbf{m}_{ref})\|_{\epsilon}^p}{\partial \delta\mathbf{m}} = \mathbf{W}_x^T \mathbf{R}_x \mathbf{W}_x (\mathbf{m}^{n-1} + \delta\mathbf{m} - \mathbf{m}_{ref}), \quad (\text{A-4})$$

where the elements of the diagonal matrix \mathbf{R}_x are given by

$$p \left\{ \left[\sum_{j=1}^N (W_x)_{ij} [m_j - (m_{ref})_j] \right]^2 + \epsilon^2 \right\}^{p/2-1} \quad (\text{A-5})$$

and

$$\begin{aligned} \frac{\partial \|\mathbf{W}_d [\mathbf{d}^{obs} - \mathbf{d}^{n-1} - \mathbf{J}(\mathbf{m}^{n-1})\delta\mathbf{m}]\|_{\epsilon}^p}{\partial \delta\mathbf{m}} \\ = \mathbf{J}^T \mathbf{W}_d^T \mathbf{R}_d \mathbf{W}_d [\mathbf{J}\delta\mathbf{m} + \mathbf{d}^{obs} - \mathbf{d}^{n-1}], \end{aligned} \quad (\text{A-6})$$

where the elements of the diagonal matrix \mathbf{R}_d are given by

$$p \left\{ \left[\sum_{j=1}^N (W_d)_{ij} [d_j^{obs} - d_j^{n-1} - J_{ij}(\mathbf{m}^{n-1})\delta m_j] \right]^2 + \epsilon^2 \right\}^{p/2-1} \quad (\text{A-7})$$

The summary of equations (A2), (A4), and (A6) and reorganization yields equation (10).

**This Page is Inserted by IFW Indexing and Scanning
Operations and is not part of the Official Record**

BEST AVAILABLE IMAGES

Defective images within this document are accurate representations of the original documents submitted by the applicant.

Defects in the images include but are not limited to the items checked:

- ☐ **BLACK BORDERS**
- ☐ **IMAGE CUT OFF AT TOP, BOTTOM OR SIDES**
- ☐ **FADED TEXT OR DRAWING**
- ☐ **BLURRED OR ILLEGIBLE TEXT OR DRAWING**
- ☐ **SKewed/SLANTED IMAGES**
- ☐ **COLOR OR BLACK AND WHITE PHOTOGRAPHS**
- ☐ **GRAY SCALE DOCUMENTS**
- ☒ **LINES OR MARKS ON ORIGINAL DOCUMENT**
- ☐ **REFERENCE(S) OR EXHIBIT(S) SUBMITTED ARE POOR QUALITY**
- ☐ **OTHER:** _____

IMAGES ARE BEST AVAILABLE COPY.

As rescanning these documents will not correct the image problems checked, please do not report these problems to the IFW Image Problem Mailbox.